Proceedings of IPC'02
4th International Pipeline Conference
September 29-October 3, 2002, Calgary, Alberta, Canada

IPC2002-27404

ADVANCED INDENTATION TECHNIQUES; NDE FOR FLOW PROPERTIES AND RESIDUAL STRESSES OF PIPELINES

Yeol Choi
Frontics, Inc.
Research Institute of Advanced materials,
Seoul National University,
Seoul 151-742, Korea

Dongil Son
Frontics, Inc.
Research Institute of Advanced materials,
Seoul National University,
Seoul 151-742, Korea

Jae-il Jang
Frontics, Inc.
Research Institute of Advanced materials,
Seoul National University,
Seoul 151-742, Korea

Joon Park
Frontics, Inc.
Research Institute of Advanced materials,
Seoul National University,
Seoul 151-742, Korea

Woo-sik Kim
Research and Development Center,
Korea Gas Corporation,
Ansan 425-150, Korea

Dongil Kwon
School of Materials Science and Engineering,
Seoul National University,
Seoul 151-742, Korea

ABSTRACT

Structural integrity assessment is indispensable for preventing catastrophic failure of industrial structures/components/facilities that are faced with time-dependent and environmentally-accelerated degradation. This diagnosis of operating components should be done periodically for safe maintenance and economical repair. However, conventional standard methods for mechanical properties have the problems of bulky specimen, destructive and complex procedure of specimen sampling. So, an advanced indentation technique has been developed as a potential method for non-destructive testing of in-field structures. This technique measures indentation load-depth curve during indentation and analyzes the mechanical properties related to deformation such as yield strength, tensile strength and work-hardening index. Also the advanced indentation technique can evaluate residual stresses based on the concept that indentation load-depth curves were shifted with the direction and the magnitude of residual stress applied to materials. In this study, we characterized the tensile properties and welding residual stress of various industrial pipeline steels through the new techniques, and the results are introduced and discussed.

INTRODUCTION

Recently, reliability diagnosis of in-service materials takes interest with frequent failure of structural components by time-dependent degradation and a severe operating environment. Especially, the operating conditions of the pipeline are more severe by the cryogenic contents and many inhomogeneous welded joints. And, the welded joint has been the initiation point of fracture by the effect of the microstructural and mechanical inhomogeneities [1]. Reliability diagnosis for safe usage based on the exact mechanical properties of local regions is indispensable.

But, conventional standard tests such as the uniaxial tensile and the fracture mechanics tests, which need the bulky standard samples, cannot be applied to the testing of in-service structure/facilities and local region such as welded joint. For examples, direct evaluation of mechanical properties of welded joint is mainly limited to the measurement of microhardness and indirect method is the testing of a bulky simulated specimen [2]. Therefore, a new mechanical testing method for locally welded joints is needed.

Also residual stress resulting from welding is one of the most important factors in reliability diagnosis. Welding thermal cycles generates inhomogeneous heating and cooling in the regions near the heat source, thus causing residual stress in the weldment. Sometimes, the value surpasses the yield strength of the welded material. It is well recognized that the presence of welding residual stresses is detrimental to the performance of the weldment. Especially, tensilely stressed region is harmful due to the susceptibility of fatigue and stress corrosion cracking [3].

Several techniques are used to measure or predict residual stress. Conventional measurement techniques can be divided into two groups; mechanical stress-relaxation and physical methods. Mechanical stress-relaxation methods including hole-

drilling and saw-cutting techniques can generally be used to evaluate residual stress quantitatively without any reference sample, but they have limitations in application due to their destructive characteristics. On the other hand, physical methods such as X-ray, neutron diffractions, magnetic Barkhausen noise and ultrasonic methods are used to analyze the residual stress non-destructively. However, they are always faced with the major problem of separating the microstructural effects from the effects of residual stress on physical parameters since the techniques are all highly sensitive to the metallurgical factors such as grain size and texture [4]. So, they often show the poor reproducibility and large scatter of testing results compared with mechanical methods. From a similar viewpoint, it is almost impossible to use the non-destructive methods for assessment of residual stresses in weldment including heat-affected zones (HAZs), which have very rapid gradient of microstructures. So a new mechanical testing method for residual stress evaluation is needed.

To overcome the limitations of both destructive/mechanical and non-destructive / physical methods, a new nondestructive/ mechanical indentation technique was developed and used for the quantitative evaluation of tensile properties and residual stresses in weldments as described in this study.

The advanced indentation technique is developed from the conventional hardness test. This technique measures the indentation load and penetration depth during loading and unloading by a spherical indenter at constant speed, instead of the direct observation and measurement of indent size in the conventional hardness test. An indentation load-depth curve is obtained from this procedure similar to the load-displacement curve from the uniaxial tensile test. This curve represents the deformation behavior of the test sample beneath the rigid ball indenter [5]. The equivalent true stress and strain identical with the flow properties from the standard uniaxial tensile test can be predicted from the analysis of indentation load-depth curve considering the indentation stress fields and deformation shape [6,7].

In this study, we evaluated the flow properties including the yield strength, work-hardening exponent and ultimate tensile strength of a girth weld joint of API X65 pipeline steel and the residual stresses of A335 P12 pipe using the advanced indentation technique.

THEORY OF ADVANCED INDENTATION

Derivation of tensile properties by advanced indentation technique

As the spherical indenter penetrates into material, mechanical deformation is divided as three stages of elastic, elastic/plastic, fully plastic [8].

A reversible deformation occurs at low load indentation. When the indentation stress fields satisfy the yield criterion, plastic zone occurs inside the material and expands to free surface. And, the contact mean pressure beneath the spherical indenter rapidly increases in this elastic/plastic region. Finally, the expanded hemi-spherical plastic zone grows into the surrounding elastic zone with a constant velocity as the indentation depth increases. The contact mean pressure slightly increases in this fully plastic region. These deformation stages are similar to the work-hardening behavior of the uniaxial tensile test except for non-homogeneity.

Research for predicting the uniaxial flow properties from indentation-induced deformation was done as described below. The raw data from the advanced indentation test is the indentation load-depth curve as shown in Fig. 1.

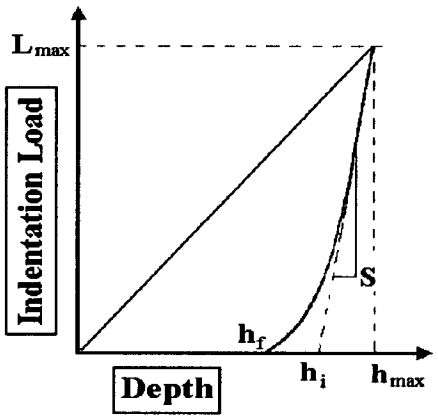

Fig. 1. Schematic graph of the indentation load-depth curve.

The equivalent stress and strain were defined in terms of the measured indentation contact parameters such as contact depth, h_c^*, indenter shape and the morphology of the deformed sample surface. And, real contact properties were determined by considering both the elastic deflection and the material pile-up around the contacting indenter as shown in Fig. 2.

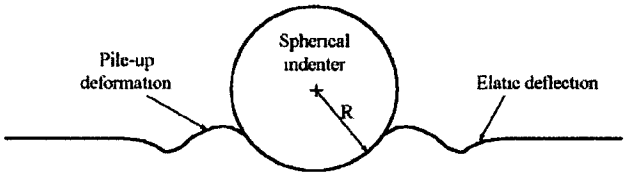

Fig. 2. Schematics of elastic and plastic deformation around indenter.

Firstly, a contact depth at maximum indentation load can be evaluated by analyzing the unloading curve with the concept of indenter geometry and elastic deflection as shown in Eq. (1) [9].

$$h_c^* = h_{max} - \omega(h_{max} - h_i) \quad (1)$$

h_i is the intercept indentation depth as shown in Fig. 1 and indenter shape parameter, ω is 0.75 for the spherical indenter. Secondly, the material pile-up around indentation enlarges the contact radius from the analysis of elastic deflection. The extent of this pile-up is determined by a constant c and the work-hardening exponent, n for steels in Eq. (2) [10,11].

$$c^2 = \frac{a^2}{a^{*2}} = \frac{5(2-n)}{2(4+n)} \quad (2)$$

a is the real contact radius and a* is the contact radius without considering the pile-up around the indent. Using the geometrical relationship of the spherical indenter, the real contact radius is expressed as Eq. (3) in terms of indenter radius, R and h_c^*.

$$a^2 = \frac{5(2-n)}{2(4+n)}(2Rh_c^* - h_c^{*2}) \quad (3)$$

The contact mean pressure, P_m is expressed as Eq. (4).

$$P_m = \frac{L_{max}}{\pi a^2} \quad (4)$$

An equivalent strain, ε_R of indentation is evaluated from the material displacement beneath the indenter along the indentation axis direction. The equivalent strain is expressed in Eq. (5) at the position of the contact radius by multiplying a fitting constant α. The value of α is used as 0.1 for various steels [6,7].

$$\varepsilon_R = \frac{\alpha}{\sqrt{1-(a/R)^2}}\frac{a}{R} \quad (5)$$

In the case of metals including structural steels, the elastic and elastic/plastic deformation stages occurred at very low indentation load. Therefore, we considered only the plastic deformation region in this study. The equivalent stress, σ_R can be evaluated using the relationship with contact mean pressure as shown Eq. (6) [6,7].

$$\frac{P_m}{\sigma_R} = \Psi \quad (6)$$

Ψ is a constraint factor for plastic deformation and the upper limit is about 3 for fully plastic deformation of steels. The exact values of work-hardening exponent, equivalent stress and strain are calculated by iteration methods [6,7].

From the analysis of each unloading curve, both equivalent stress and strain values are determined. The stress and strain relation is fitted as the power-type Hollomon equation expressing work-hardening behavior. The fitted curve was extrapolated to initial yield and ultimate tensile regions. Then, yield strength was evaluated by inputting yield strain to the Hollomon equation. The ultimate tensile strength was evaluated using the concept that uniform elongation is equal to work-hardening exponent.

Evaluation of residual stress using advanced indentation technique

Indentation hardness was used as a parameter of the residual stress in initial studies [12]. However, the variations in the apparent hardness with a change in the residual stress have been identified as an artifact of erroneous optical measurements of the indentation mark. Recently, the intrinsic hardness has been reported as constant regardless of the residual stress in studies using fine observations of the indentation mark [13,14] by scanning electron or atomic force microscopes. Therefore, the change in contact morphologies with residual stress was modeled for constant maximum indentation depth assuming the independence of the intrinsic hardness and the residual stress [15].

The change in indentation deformation caused by the residual stress was identified in the indentation loading curve shown in Figs. 3 and 4. The applied load of the tensile stressed state is lower than that of a stress-free state for the same maximum indentation depth [13-15]. In other words, the maximum indentation depth desired is reached at a smaller indentation load in a tensile stressed film, because a residual-stress-induced normal load acts as an additive load to the applied load. Therefore, the residual stress can be evaluated by analyzing the residual-stress-induced normal load.

The detailed changes in contact morphology can be explained from the schematic diagram shown in Fig. 5 (a) and (b). The residual stress is relaxed for a tensile stressed specimen maintaining the constant maximum depth, h_i, as the stress relaxation pushes the indenter out from the surface. However, the pushing force appears as increases in the applied load ($L_T \rightarrow L_0$) and the contact depth ($h_c^T \rightarrow h_c$), because the maximum depth is held constant. The indentation load and maximum depth for the tensile stressed state (L_T, h_i) is equivalent to those in the relaxed state (L_0, h_i). Thus, the relationship between the two states can be expressed as

$$L_0 = L_T + L_{res} \quad (7)$$

In the compressive stress state, the applied load and contact depth decrease by stress relaxation under the maximum-depth-controlled path. Furthermore, this decreasing portion of the applied load was the residual-stress-induced normal load, L_{res}. Therefore, the residual stress in a welded joint can be evaluated by dividing L_{res} by the contact area, A_c, regardless of the stress state [15]:

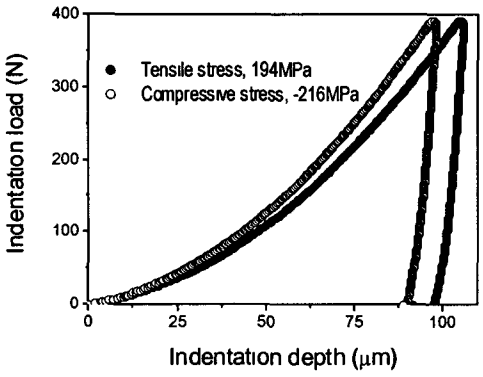

Fig. 3. The variation of indentation load-depth curves with the magnitude of applied residual stress [authors? unpublished data].

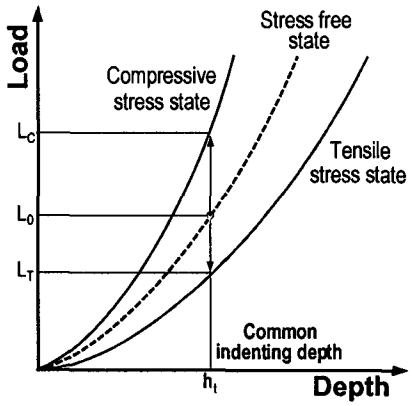

Fig. 4. Variation of the indentation loading curves with the changes in the stress states [13-15].

$$\sigma_{res} = L_{res} / A_c \tag{8}$$

To evaluate the stress values from several indentation load steps, we performed multiple indentations and calculated the contact area directly from the partial unloading curve at each analyzed load. In the instrumented indentation test, the contact area is determined by unloading curve analysis as shown in Fig. 1. By differentiation of the power-law fitted unloading curve at maximum indentation depth, we can get the contact depth as shown in Eq. (1). [9] And contact area, A_c calculated from the contact depth based on the geometry of the Vickers indenter.

$$A_c = 24.5 h_c^2 \tag{9}$$

Consequently, residual stress was calculated from the analyzed contact area in Eq. (9) and the measured load change, L_{res} by the effect of residual stress shown in Eq. (7).

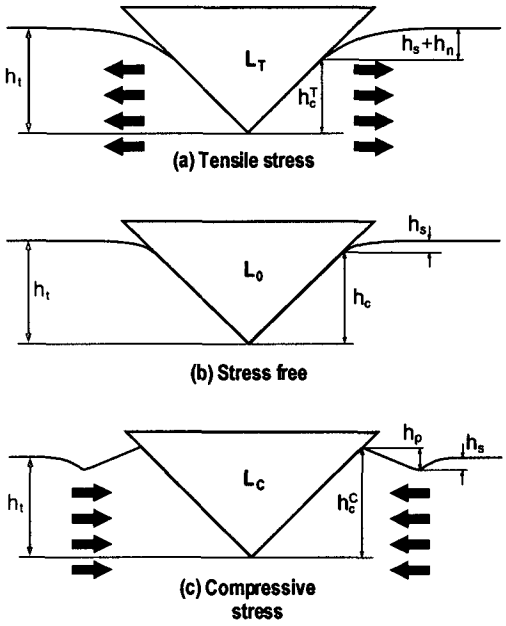

Fig. 5. Theoretical surface morphologies around the contact for (a) tensile stress, (b) stress-free and (c) compressive stress states.

EXPERIMENTAL PROCEDURES

Sample Preparation

Natural gas transmission pipe was made by welding API X65 steel plates. The diameter and thickness of the pipe were 30 inch and 17.5mm, respectively. Seam welded pipe was welded each other circumferentially. The chemical compositions of API X65 base metal are summarized in Table 1.

Table 1. Chemical composition of API X65 and A335 P12 used in this work as the base material (wt %).

Comp. (wt%)	C	P	Mn	S	Si	Cr	Mo	Fe
API X65	0.08	0.019	1 45	0.003	0.31	-	-	Bal
A335 P12	0.08	0.01	0.45	0.01	0 31	1.15	0.55	Bal

The circumferential girth weld joint was made by Gas Tungsten Arc Welding (GTAW) and Shielded Metal Arc Welding (SMAW) process with V-groove configuration. The

welding materials and welding conditions are summarized in Table 2. A mechanical test sample was obtained from the circumferential weld joint with the size of 10mm×50mm×17.5mm. The sample was ground with emery paper and finally polished with 1μm diamond paste.

The sample used in residual stress evaluation was obtained from a girth weld joint of cold reheater pipeline from a fossil power plant. A335 P12 steel of a 17.9 mm thickness, which is the base metal of the pipe, was machined into X-groove configuration and welded by gas tungsten arc welding (GTAW) at first and shielded metal arc welding (SMAW) process. Welding was carried out under the same conditions as those used during the construction of the plant facilities. Tables 1 and 2 list the chemical composition of A335 P12 and the used welding condition, respectively. In addition, no significant defects were found in the completed weldments by the non-destructive X-ray examination. Additionally, post weld heat treatment (PWHT) was conducted on part of the samples for residual stress relaxation. The results taken from the PWHT specimens were compared with those from the as-welded specimens.

Table 2. Welding Materials and conditions for girth welded joint.

Materials	Welding Method	Filler Metal	Groove shape
API X65	GTAW+ SMAW	AWS ER70S-G AWS E9016-G	V
A335 P12	GTAW+ SMAW	AWS ER80S-G AWS E8016-G	X

Test Procedures

The testing machine was the Advanced Indentation System ™ made by Frontics, Inc. The maximum capacity of the load sensor is 300kgf and maximum range of displacement sensor is 3mm. The accuracy of sensors are 300gf and 0.2μm, respectively. The spherical indenter is a tungsten ball of 0.5mm radius. The testing modes for true stress-strain relationship can be selected as maximum load and maximum depth controlling methods. And, maximum depth controlling mode for same equivalent strain was used in this study.

In the experiment for flow properties, the maximum indentation depth was 250μm, and 25 partial unloadings down to 70% of maximum load at each point were applied. Loading and unloading speed was 0.2mm/min. The advanced indentation test was done along the 3 lines of the outer, middle and inner part of the weld joint thickness. The distance between indentation marks was 4mm to avoid the superposition of plastic deformation fields. The indentation load-depth curve obtained from the multiple indentation technique was analyzed to determine flow properties including yield strength, work-hardening exponent and ultimate tensile strength based on the theoretical background. Indentation load-depth curve with slippage at low load region was treated as testing error and excluded from the analysis. And then, the microstructure of the tested sample was observed optically. The regions of weld metal, HAZ and base metal were distinguished using the optical metallography and conventional research of the variation of microhardness.

In order to evaluate the residual stress in the weldment, two kinds of testing methods were performed at both PWHT and as-welded specimens; nondestructive indentation and destructive saw-cutting tests. Results from the indentation tests were compared with those from saw-cutting method for validation of the advanced indentation method.

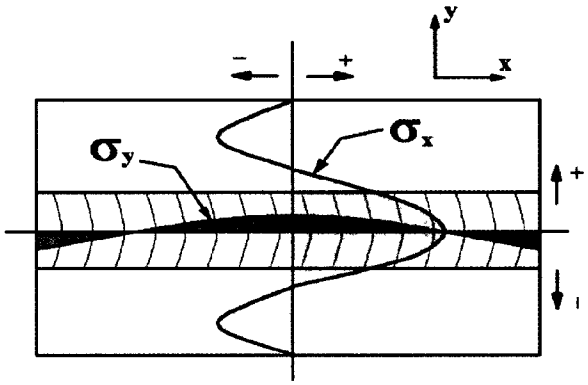

Fig. 6. Schematic illustration of typical distribution of longitudinal (σ_x) and transverse (σ_y) residual stresses in a butt weld.

To measure the distribution of the longitudinal residual stress (σ_x in Fig. 6) using the saw-cutting technique, strain gauges were attached along the distance from weld centerline. The gauges provided information about the relaxed residual stress value during cutting. Signals from strain gauges were obtained from a multi-channel amplifier. Samples were manually cut using a cutting saw, because any auto-cutter generates heat which could change microstructures of materials and give damage to the attached strain gauge. The relaxed strain values were easily converted to residual stress by multiplying the elastic modulus. The indentation tests were performed before and after cutting. Indentation arrays using Vickers indenter was made on the polished surface near the cutting line at intervals of 5 mm. Maximum load and loading-unloading speed were 50 kgf and 0.5 mm/min, respectively. After cutting, indentation tests were also performed at the nearest location (3mm) from the cut line, the results of which were used as reference or stress-free states. Residual stress is calculated by comparison of two indentation tests before and

after cutting. Tested sample is shown in Fig. 7.

Fig. 7. Actual views of tested specimens, on which both saw-cutting and indentation were performed.

RESULTS AND DISCUSSION

Tensile Properties of Three Microstructurally Characteristic Regions

The boundary between heat-affected zone (HAZ) and base metal was identified 7mm from the fusion line using optical metallography and microhardness data for girth welded joint. The multiple indentation load-depth curves from three regions were superposed as shown in Fig. 8.

Comparing the maximum indentation loads at the same indentation depth, it was found the material resistance to deformation was high as the sequence of weld metal, base metal and HAZ. The true stress-strain behaviors were obtained from each indentation point. Generally, higher yield strengths were evaluated for weld metal and base metal than that of HAZ as expected from indentation load-depth curve. Especially, the yield strength of HAZ was lower than base metal as shown in Fig. 9. It is due to the softening phenomenon during welding process [10], generally observed in HAZ of thermo-mechanical control processed (TMCP) steel such as the steel used in this study. And, HAZ can be identified as the weakest point for plastic deformation. The variation of yield strengths for outer, middle and inner lines are shown in Fig. 10 for the entire girth weld joint. The left part of the middle line has missing data due to the testing error by indenter slippage. The yield strengths of HAZ in the inner line were lower than those of HAZ in outer and middle lines. This phenomenon was explained by the annealing heat treatment of the constant heat input from outer welding paths.

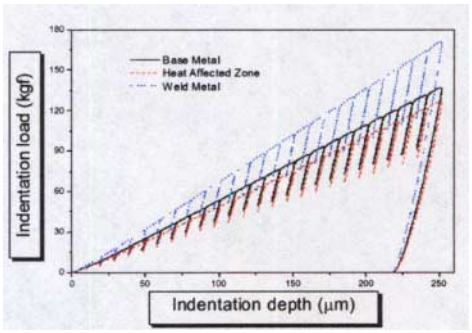

Fig. 8. Variation of indentation load-depth with the change of microstructures.

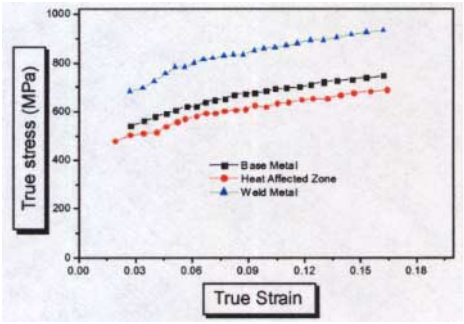

Fig. 9. The difference of flow properties with the change of microstructures.

Next, to assess the reliability of the advanced indentation test, the true stress-strain properties of base metal from the advanced indentation test was compared with the result from the uniaxial tensile test. The uniaxial tensile testing was done using the thin plate specimens obtained from 3 parts of thickness direction. The gauge length, width and thickness of the sample were 25mm×6mm×4mm. The yield strengths of outer, middle and inner lines were 490, 440 and 495MPa, respectively. And, the ultimate tensile strengths of outer, middle and inner lines were 628, 535 and 625MPa, respectively. The flow properties from advanced indentation testing are summarized below. The yield strengths of outer, middle and inner lines from advanced indentation were 453, 451 and 467MPa, respectively. The ultimate tensile strengths of outer, middle and inner lines were 718, 726 and 683MPa, respectively. Based upon the comparison of the test results, it was determined that the advanced indentation test can be

successfully used for nondestructive evaluation of tensile properties.

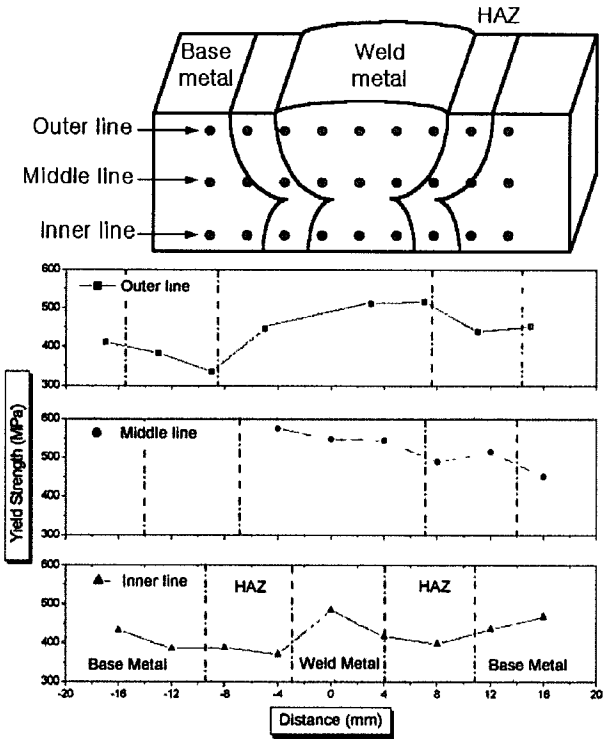

Fig. 10. Variation of the yield strengths for outer, middle and inner lines of the girth weld joint

Comparison of Residual Stresses between Saw-Cutting Technique and New Indentation Technique

Figure 11 summarizes the results obtained from saw-cutting tests and the indentation technique showing the distribution of longitudinal residual stresses of both PWHT and as-welded specimens. The saw-cutting tests shows the maximum residual stress existing near the weld centerline in as-welded specimen, i.e. specimen before PWHT, is up to 250 MPa, which is over the minimum required yield strength (220 MPa) of the A335 P12 steel used as base metal of the pipe. The high residual stress disappeared in PWHT specimen, as expected. So, it could be recognized that, post weld heat treatment is very effective in relaxing residual stresses.

The variation in residual stresses measured by indentation tests also can be shown in Fig. 11. The variation tendencies of residual stresses are similar to those in saw-cutting tests. High residual stresses observed in as-welded specimen were clearly relaxed.

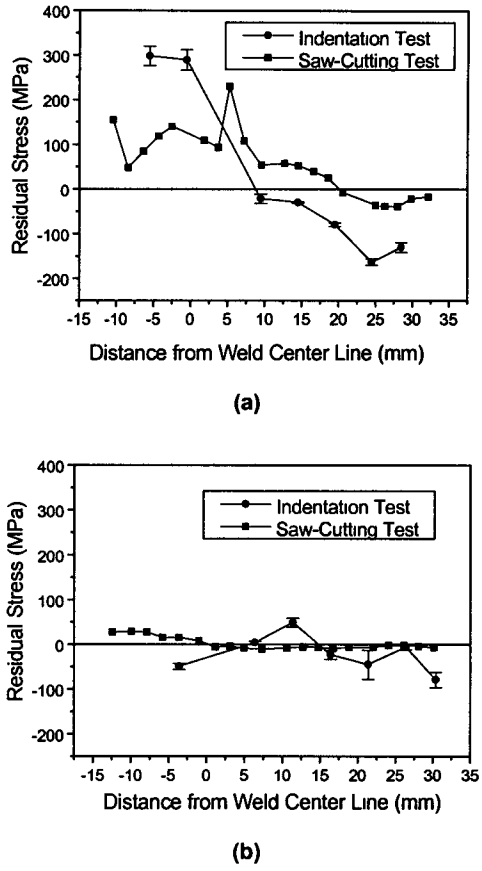

Fig. 11. Direct comparison of residual stresses measured by indentation technique with those obtained from saw-cutting tests; (a) as-welded specimen (before PWHT) and (b) PWHT specimen.

Comparing residual stresses measured by the indentation test with those measured by the saw-cutting test, there was a little difference in stress values. The reason of difference is due to the difference in the kind of residual stresses measured in each test. The stress measured by the indentation technique is bi-axial stress including both longitudinal (σ_x in Fig. 6) and transverse stress (σ_y in Fig. 6) while residual stresses obtained from the saw-cutting tests are just longitudinal stress. From all above results, it could be concluded that the advanced indentation technique can be applied to non-destructive evaluation of residual welding stresses in industrial facility piping.

CONCLUSIONS

The advanced indentation technique was used to evaluate the variation of the flow properties of an API X 65 girth welded

joint and residual stress in an A335 P12 steels girth welded joint.

(1) The true stress-strain curves for the welded joint were evaluated based on the analysis of equivalent stress and strain considering the deformation behavior beneath the spherical indenter and indentation stress field.
(2) The degree of deformation resistance was compared for weld metal, HAZ and base metal with indentation load-depth curve and evaluated yield strength. Weld metal was identified as the highest value among the three regions. And, HAZ had the lowest value. Therefore, HAZ was the weakest point for plastic deformation.
(3) The yield strength and work-hardening exponent of API X 65 base metal was nearly consistent with the results from the uniaxial tensile test.
(4) By comparing with the results from conventional saw-cutting tests, it was found that the indentation tests could be used for quantitative non-destructive assessment of welding residual stresses in industrial facilities or structures.

REFERENCES

[1] Kim, B.C., Lee, S., Kim, N.J., and Lee, D.Y., 1991, "Microstructure and Local Brittle Zone Phenomena on High-Strength Low-Alloy Steel Welds," Metallurgical Transactions A, Vol. 22A, pp.139-149.

[2] Rosenthal, D., 1946, "The Theory of Moving Sources of Heat and Its Application to Metal Treatments," Transaction of ASME, Vol. 68, pp.849-860.

[3] Noyan, I. C. and Cohen, J. B., 1987, "Residual Stresses," Springer-Verlag, New York.

[4] Lu, J., James, M.R., and Mordfin, L., 1996, "Handbook of measurement of residual stresses, " Society for Experimental Mechanics, Inc., Lu, J. (Ed.), Fairmont Press, Inc., Lilburn, GA, Ch. 8.

[5] Field, J.S. and Swian, M.V., 1995, "Determining the Mechanical Properties of Small Volumes of Material from Submicrometer Spherical Indenter," Journal of Materials Research, Vol. 10, pp. 101-112.

[6] Ahn, J.-H., Choi, Y., and Kwon, D., 2000, "Evaluation of Plastic Flow Properties of Materials through the Analysis of Indentation Load-Depth Curve," Journal of the Korean Institute of Metal and Materials, Vol. 38, pp. 1606-1611.

[7] Ahn, J.-H. and Kwon, D., 2001, "Derivation of plastic stress-strain relationship from ball indentation: Examination of strain definition and pileup effect," J. Mater. Res., Vol. 16, pp. 3170-3178.

[8] Francis, F.A., 1976, "Phenomenological Analysis of Plastic Spherical Indentation," Journal of Engineering Materials and Technology Transaction ASME, Vol. 98, pp. 272-281.

[9] Oliver, W.C., and Pharr, G.M., 1992, "An Improved Technique for Determining Hardness and Elastic Modulus using Load and Displacement Sensing Indentation Experiment," Journal of Materials Research, Vol. 7, pp. 1564-1583.

[10] Norbury, A.L., and Samuel, T., 1928, "The Recovery and Sinking-in or Piling-up of Material in the Brinell Test, and the Effects of These Factors on the Correlation of the Brinell with Certain Other Hardness Tests," Journal of Iron and Steel Institute, Vol. 117, pp. 673-687.

[11] Hill, R., F.R.S., Storåkers, B., and Zdunek, A.B., 1989, "A theoretical Study of the Brinell Hardness Test," Proceedings of Royal Society in London, Vol. A423, pp. 301-330.

[12] LaFontaine, W. R., Paszkiet, C. A., Korhonen, M. A. and Li, C.-Y., 1991, "Residual stress measurements of thin aluminum metallizations by continuous indentation and x-ray stress measurement techniques", J. Mater. Res., Vol. 6, pp. 2084-2090.

[13] Tsui, T. Y., Oliver, W. C. and Pharr, G. M., 1996, "Influences of stress on the measurement of mechanical properties using nanoindentation: Part I. Experimental studies in an aluminum alloy", J. Mater. Res., Vol. 11, pp. 752-759.

[14] Suresh, S. and Giannakopoulos, A.E., 1998, "A New Method for Estimating Residual Stresses by Instrumented Sharp Indentation," Acta mater., Vol. 46, pp. 5755-5767.

[15] Lee, Y.-H. and Kwon, D., 2002, "Residual stresses in DLC/Si and Au/Si systems: Application of a stress-relaxation model to the nanoindentation technique," J. Mater. Res. Vol 17, pp. 901-906.